Structural Eng. / Earthquake Eng. Vol. 5. No. 1, 193s-203s. April 1988
Japan Society of Civil Engineers (Proc. of JSCE No. 392/I-9)

GALLOPING OF STRUCTURE WITH TWO CLOSELY-SPACED NATURAL FREQUENCIES

By Phoonsak PHEINSUSOM and Yozo FUJINO***

Certain structures have the vibration modes of closely-spaced natural frequencies. The galloping behaviour of such a structure is studied. A cable-stayed bridge tower whose the natural frequency of the in-plane second mode is close to that of the in-plane first mode is employed as the case study. The structure is modeled as a linear two-degree-of-freedom system with proportional damping, and nonlinear quasi-steady wind force is assumed. An asymptotic modal analysis on galloping is conducted. The results indicate that the galloping of this tower is the steady-state motion either in one of the two modes, depending upon the initial disturbances, and that the coexistence of two modes in galloping, i. e. multi-mode galloping, is unstable. However, for structures with certain properties, e. g. unsymmetrically distributed mass, only the multi-mode galloping is stable. These results agree well with the observations in wind tunnel experiments.

Keywords : bridge tower, galloping, multi-modal response, nonlinear asymptotic analysis, vibration mode, wind tunnel experiment

1. INTRODUCTION

Galloping is one of the most important wind-induced oscillation problems of the flexible structure. The usual assumption to analyze this phenomenon is that galloping is a vibration of single uncoupled mode in the direction normal to wind. Analysis using this assumption was carried out in great detail by Novak[1] and others.

Galloping of two-degree-of-freedom system allowing vertical and torsional motions was explored by Blevins and Iwan[2]. They concluded that there is strong interaction between vertical and torsional motions when two natural frequencies are close to an integer multiple of each other. This interaction is greatest when two natural frequencies are nearly equal, i. e. the torsional motion noticeably coexists with the vertical galloping.

The tower of the Higashi-Kobe cable-stayed bridge has an interesting property that the circular natural frequency of the in-plane second mode, ω_2 is close to that of the in-plane first mode, ω_1 as shown in Fig. 1. The galloping behaviour of this tower with the proposed rectangular cross-section in uniform wind flowing in the direction of the bridge axis has been experimentally studied in the wind tunnel using its three dimensional 1 : 100 scaled model[3]. The tower's galloping was the steady-state motion either in the first mode or in the second mode depending upon the initial disturbances given to the tower model. The relation between wind velocity and modal amplitudes at the top of tower obtained from this experiment is presented in Fig. 2. The studies by Phoonsak et al.[4)~6)], which are our primary works on this topic, showed that the nonlinear asymptotic analysis can well explains these observations. However, it is interesting to note that the coexistence of both the first mode and the second mode motions in galloping, i. e. multi-mode galloping,

* Member of JSCE, M. Eng., Graduate student, Dept. of Civil Eng., Univ. of Tokyo (Bunkyo-ku, Tokyo 113)
** Member of JSCE, Ph. D., Assoc. Prof., Eng. Res. Inst., Fac. of Eng., Univ. Of Tokyo (Bunkyo-ku, Tokyo 113)

is not a steady-state motion as shown in Fig. 3. These observations curiously differ from the results obtained in Ref. 2).

Shiraishi et al.[7] also performed experiments using a scaled three dimensional model of this tower and similar results were obtained. Note that their study concerns the galloping suppression of the tower and it indicates that galloping of this tower is effectively suppressed by adding corner-cut to the original rectangular cross-section. The cross-section with corner-cut is employed as the final design proposal.

The present paper, which is a continuous work from Ref. 4), 5) and 6), attempts to explain the galloping behaviour of the structure with two closely-spaced natural frequencies. Focus is placed on the modal selection during galloping. The modal equations of motion are firstly formulated under the assumptions of linear elastic structure and nonlinear quasi-steady wind forces. Solving these nonlinear coupled equations of motion by perturbation method, the modal selection in galloping of this kind of structure is studied. Next, the conditions of the existence of steady-state multi-mode galloping is examined. Finally, the analytical results are compared with observations from the wind tunnel experiments.

2. EQUATIONS OF MOTION

Consider the continuous structure, for example the bridge tower shown in Fig. 1, subjected to the smooth wind flow. The structure is assumed to be a linear elastic proportionally-damped system. Using the conventional modal analysis, response of the structure in the direction normal to wind, $Y(x, t)$ can be expressed as

$$Y(x, t)=\sum_{i}^{n} \gamma_i(x)y_i(t) \quad \cdots\cdots (1)$$

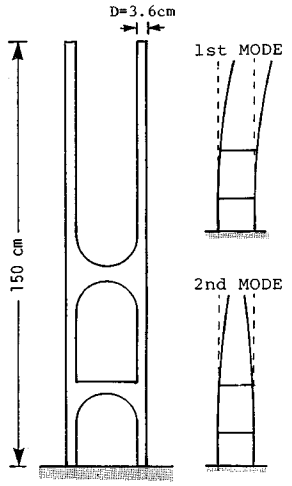

Modal circular natural frequencies
$\omega_1=43.2$ rad/s, $\omega_2=47.4$ rad/s.
Modal critical damping ratios
$\xi_1=0.0016$, $\xi_2=0.0014$.
Modal mass ratios
$n_1=n_2=0.00027$.
Wind force coefficients of 2 : 3 rectangular cross-section
$A_1=6.6$, $A_2=0.0$, $A_3=-118.9$.
Modal Integrals (γ_i : i-th mode shape)

$\int \gamma_1^3 dx=19.7$, $\int \gamma_2^3 dx=19.7$,
$\int \gamma_1^2 dx=-23.3$, $\int \gamma_2^2 dx=0.0$,
$\int \gamma_1^2\gamma_2 dx=0.0$, $\int \gamma_1\gamma_2^2 dx=-25.4$,
$\int \gamma_1 dx=30.7$, $\int \gamma_2 dx=38.9$,
$\int \gamma_1^2\gamma_2 dx=0.0$, $\int \gamma_1\gamma_2^2 dx=0.0$,
$\int \gamma_1^2\gamma_2^2 dx=34.1$.

Fig. 1 Higashi-Kobe bridge tower's model with mode shapes and modal properties.

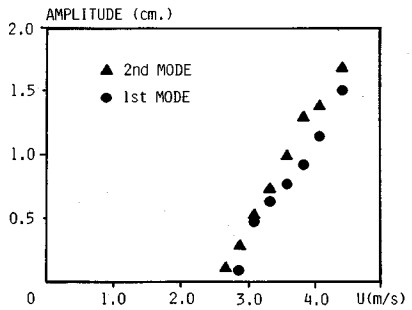

Fig. 2 Amplitude-Wind velocity relation of tower (wind tunnel experiment).

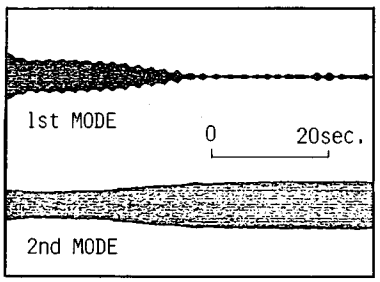

Fig. 3 Example of steady-state response of tower (the second mode galloping).

where $\gamma_i(x)=i$-th mode shape and $y_i(t)=i$-th modal response.

The i-th modal equation of motion can be written as

$$\ddot{y}_i+2\,\xi_i\omega_i\dot{y}_i+\omega_i^2 y_i=\int F_Y(x,\,t)\gamma_i(x)dx\,/\left(\int m(x)\gamma_i^2(x)dx\right) \quad (2)$$

where ξ_i=critical damping ratio of i-th mode, ω_i=circular natural frequency of i-th mode, $m(x)$=mass of the structure per unit length, $F_Y(x,\,t)$=external force and dot denotes the differentiation with respect to time t.

In this study, the wind force is assumed to be quasi-steady. Using this assumption, the galloping force $F_Y(x,\,t)$ may be written in a polynomial form as

$$F_Y(x,\,t)=0.5\,\rho U^2 D\left\{A_1\left(\frac{\dot{Y}}{U}\right)+A_2\left(\frac{\dot{Y}}{U}\right)^2+\cdots+A_j\left(\frac{\dot{Y}}{U}\right)^j+\cdots+A_n\left(\frac{\dot{Y}}{U}\right)^n\right\} \quad (3)$$

where ρ=air density, U=uniform wind velocity, D=characteristic dimension of structure and A_j=wind force coefficients.

Using the quasi-steady wind force assumes that the wind force on the cross-section in a flow at any time is identical with the force on that cross-section in a steady flow at the same relative angle of attack and wind velocity. This assumption has been found to be a useful approximation as long as the onset wind velocity of galloping is much higher than the onset wind velocity of vortex shedding. The applicability of quasi-steady wind force assumption on this problem will be discussed later.

Substitution of Eqs. (1) and (3) into Eq. (2) leads to the set of modal equations of motion. The right hand side of these equations, which represents aeroelastic force, is nonlinear and coupled while the left hand side, which represents structural properties, is linear and uncoupled. Difficulty in solving this set of equations depends upon the number of modes included and the order of polynomial in aeroelastic forces. From the wind tunnel experiment, tower's response was found to practically consist of the in-plane first and the in-plane second modes as shown in Fig. 2. Therefore, only the first two modes are employed in the following analysis. Furthermore, to simplify the analysis, up to the third order nonlinear terms of the self-excited force in Eq. (3) are considered. Neglecting the higher order nonlinear terms will, of course, lessen the accuracy of the solutions; however, the solutions will not be dramatically changed. Then, considering only up to the third order nonlinear terms in Eq. (3) is believed to be adequate for the analysis focusing the modal selection during galloping. That is

$$Y(x,\,t)=\gamma_1(x)y_1(t)+\gamma_2(x)y_2(t) \quad (4)$$

$$F_Y(x,\,t)=0.5\,\rho U^2 D\left\{A_1\left(\frac{\dot{Y}}{U}\right)+A_2\left(\frac{\dot{Y}}{U}\right)^2+A_3\left(\frac{\dot{Y}}{U}\right)^3\right\} \quad (5)$$

Then the modal equations of motion are

$$\ddot{y}_1+\omega_1^2 y_1=\alpha_1\dot{y}_1+\alpha_2\dot{y}_1^2+\alpha_3\dot{y}_1\dot{y}_2+\alpha_4\dot{y}_2^2+\alpha_5\dot{y}_1^3+\alpha_6\dot{y}_1^2\dot{y}_2+\alpha_7\dot{y}_1\dot{y}_2^2+\alpha_8\dot{y}_2^3 \quad (6\cdot a)$$

$$\ddot{y}_2+\omega_2^2 y_2=\beta_1\dot{y}_2+\beta_2\dot{y}_1^2+\beta_3\dot{y}_1\dot{y}_2+\beta_4\dot{y}_2^2+\beta_5\dot{y}_1^3+\beta_6\dot{y}_1^2\dot{y}_2+\beta_7\dot{y}_1\dot{y}_2^2+\beta_8\dot{y}_2^3 \quad (6\cdot b)$$

where

$$\alpha_1=-2\,\xi_1\omega_1+2\,n_1UA_1\int\gamma_1^2dx/D,\qquad \beta_1=-2\,\xi_2\omega_2+2\,n_2UA_1\int\gamma_2^2dx/D \quad (7\cdot a,\ 7\cdot b)$$

$$\alpha_2=2\,n_1A_2\int\gamma_1^3dx/D,\qquad \beta_2=2\,n_2A_2\int\gamma_1^2\gamma_2dx/D \quad (7\cdot c,\ 7\cdot d)$$

$$\alpha_3=4\,n_1A_2\int\gamma_1^2\gamma_2dx/D,\qquad \beta_3=4\,n_2A_2\int\gamma_1\gamma_2^2dx/D \quad (7\cdot e,\ 7\cdot f)$$

$$\alpha_4=2\,n_1A_2\int\gamma_1\gamma_2^2dx/D,\qquad \beta_4=2\,n_2A_2\int\gamma_2^3dx/D \quad (7\cdot g,\ 7\cdot h)$$

$$\alpha_5=2\,n_1A_3\int\gamma_1^4dx/(DU),\qquad \beta_5=2\,n_2A_3\int\gamma_1^3\gamma_2dx/(DU) \quad (7\cdot i,\ 7\cdot j)$$

$$\alpha_6=6\,n_1A_3\int\gamma_1^3\gamma_2dx/(DU),\qquad \beta_6=6\,n_2A_3\int\gamma_1^2\gamma_2^2dx/(DU) \quad (7\cdot k,\ 7\cdot l)$$

$$\alpha_7=6\,n_1A_3\int\gamma_1^2\gamma_2^2dx/(DU),\qquad \beta_7=6\,n_2A_3\int\gamma_1\gamma_2^3dx/(DU)\cdots\cdots(7\cdot m,\ 7\cdot n)$$

$$\alpha_8=2\,n_1A_3\int\gamma_1\gamma_2^3dx/(DU),\qquad \beta_8=2\,n_2A_3\int\gamma_2^4dx/(DU)\cdots\cdots(7\cdot p,\ 7\cdot q)$$

$$n_1=\rho D^2/\left(4\int m(x)\gamma_1^2(x)dx\right),\qquad n_2=\rho D^2/\left(4\int m(x)\gamma_2^2(x)dx\right)\cdots\cdots(7\cdot r,\ 7\cdot s)$$

3. ASYMPTOTIC SOLUTION FOR STRUCTURE WITH TWO CLOSELY-SPACED NATURAL FREQUENCIES

In order to solve the coupled nonlinear differential Eqs. (6·a) and (6·b), the nonlinear terms are assumed to be very small which can be characterized by a parameter ε. The solution is assumed as

$$y_1(t)=a_1(t)\cos\Omega_1+\varepsilon y_{11}(a_1,a_2,\Omega_1,\Omega_2)\cdots\cdots(8\cdot a)$$

$$y_2(t)=a_2(t)\cos\Omega_2+\varepsilon y_{22}(a_1,a_2,\Omega_1,\Omega_2)\cdots\cdots(8\cdot b)$$

where $\Omega_1=\omega_1t-\delta_1(t)$, $\Omega_2=\omega_2t-\delta_1(t)-\delta_2(t)$.

The variables a_1, a_2, Ω_1 and Ω_2 are assumed to be slowly varying functions of time t such that

$$\dot y_1=-\omega_1a_1\sin\Omega_1+\varepsilon\dot y_{11}\cdots\cdots(9\cdot a)$$

$$\dot y_2=-\omega_2a_2\sin\Omega_2+\varepsilon\dot y_{22}\cdots\cdots(9\cdot b)$$

This implies that

$$\dot a_1\cos\Omega_1+a_1\dot\delta_1\sin\Omega_1=0\cdots\cdots(10)$$

$$\dot a_2\cos\Omega_2+a_2(\dot\delta_1+\dot\delta_2)\sin\Omega_2=0\cdots\cdots(11)$$

Substituting Eqs. (8) and (9) into Eqs. (6) and considering only the terms with the same order as ε, one obtains

$$\begin{aligned}\ddot y_{11}+\omega_1^2y_{11}=&[\omega_1\dot a_1-\omega_1a_1\alpha_1-0.75\,\omega_1^3a_1^3\alpha_5-0.5\,\omega_1\omega_2^2a_1a_2^2\alpha_7]\sin\Omega_1-\omega_1a_1\dot\delta_1\cos\Omega_1\\&-[0.5\,\omega_1^2\omega_2a_1^2a_2\alpha_6+0.75\,\omega_2^3a_2^3\alpha_8]\sin\Omega_2+0.5\,\omega_1^2a_1^2\alpha_2+0.5\,\omega_2^2a_2^2\alpha_4\\&-0.5\,\omega_1^2a_1^2\alpha_2\cos2\Omega_1-0.5\,\omega_2^2a_2^2\alpha_4\cos2\Omega_2\\&+0.5\,\omega_1\omega_2a_1a_2\alpha_3[\cos(\Omega_1-\Omega_2)-\cos(\Omega_1+\Omega_2)]\\&+0.25\,\omega_1^3a_1^3\alpha_5\sin3\Omega_1+0.25\,\omega_2^3a_2^3\alpha_8\sin3\Omega_2\\&+0.25\,\omega_1^2\omega_2a_1^2a_2\alpha_6[\sin(\Omega_2+2\Omega_1)+\sin(\Omega_2-2\Omega_1)]\\&+0.25\,\omega_1\omega_2^2a_1a_2^2\alpha_7[\sin(\Omega_1+2\Omega_2)+\sin(\Omega_1-2\Omega_2)]\cdots\cdots(12\cdot a)\end{aligned}$$

$$\begin{aligned}\ddot y_{22}+\omega_2^2y_{22}=&[\omega_2\dot a_2-\omega_2a_2\beta_1-0.75\,\omega_2^3a_2^3\beta_8-0.5\,\omega_1^2\omega_2a_1^2a_2\beta_6]\sin\Omega_2-\omega_2a_2(\dot\delta_1+\dot\delta_2)\cos\Omega_2\\&-[0.5\,\omega_1\omega_2^2a_1a_2^2\beta_7+0.75\,\omega_1^3a_1^3\beta_5]\sin\Omega_1+0.5\,\omega_1^2a_1^2\beta_2+0.5\,\omega_2^2a_2^2\beta_4\\&-0.5\,\omega_1^2a_1^2\beta_2\cos2\Omega_1-0.5\,\omega_2^2a_2^2\beta_4\cos2\Omega_2\\&+0.5\,\omega_1\omega_2a_1a_2\beta_3[\cos(\Omega_1-\Omega_2)-\cos(\Omega_1+\Omega_2)]\\&+0.25\,\omega_1^3a_1^3\beta_5\sin3\Omega_1+0.25\,\omega_2^3a_2^3\beta_8\sin3\Omega_2\\&+0.25\,\omega_1^2\omega_2a_1^2a_2\beta_6[\sin(\Omega_2+2\Omega_1)+\sin(\Omega_2-2\Omega_1)]\\&+0.25\,\omega_1\omega_2^2a_1a_2^2\beta_7[\sin(\Omega_1+2\Omega_2)+\sin(\Omega_1-2\Omega_2)]\cdots\cdots(12\cdot b)\end{aligned}$$

The terms whose frequency is nearly ω_1 in Eq. (12·a) and those whose frequency is nearly ω_2 in Eq. (12·b) will give unbounded solution for any values of ω_1 and ω_2. These terms which are called secular terms must be eliminated in order to obtain bounded solution of a_1 and a_2.

The case that the second mode frequency is close to that of the first mode is considered. To express quantitatively the closeness between these two natural frequencies, the detuning parameter σ is introduced as

$$\omega_2=\omega_1+\varepsilon\sigma\cdots\cdots(13)$$

Then the terms with Ω_1, Ω_2, $(\Omega_1-2\Omega_2)$ and $(\Omega_2-2\Omega_1)$ in Eqs. (12) are secular terms.

Performing certain algebraic operations and averaging Eqs. (10) and (11) along with the equations which result from the elimination of secular terms in Eqs. (12) lead to the following set of equations.

$$\begin{aligned}\dot a_1=&0.5\,a_1\alpha_1+0.375\,\omega_1^2a_1^3\alpha_5+0.25\,\omega_2^2a_1a_2^2\alpha_7[1+0.5\cos2\lambda]\\&+0.375[\omega_1\omega_2a_1^2a_2\alpha_6+\omega_2^3a_2^3\alpha_8/\omega_1]\cos\lambda\cdots\cdots(14)\end{aligned}$$

Table 1 Possible Solution Sets of Eqs. (14) ~ (16).

PARAMETERS \ SOLUTION SETS	$a_1 \neq 0,\ a_2 \neq 0$	$a_1 = 0,\ a_2 \neq 0$	$a_1 \neq 0,\ a_2 = 0$	$a_1 = 0,\ a_2 = 0$
$\beta_5 = 0,\ \alpha_8 = 0$	EXISTS	EXISTS	EXISTS	EXISTS
$\beta_5 \neq 0,\ \alpha_8 = 0$	EXISTS	DOES NOT EXIST	EXISTS	EXISTS
$\beta_5 = 0,\ \alpha_8 \neq 0$	EXISTS	EXISTS	DOES NOT EXIST	EXISTS
$\beta_5 \neq 0,\ \alpha_8 \neq 0$	EXISTS	DOES NOT EXIST	DOES NOT EXIST	EXISTS

$$\dot{a}_2 = 0.5\, a_2\beta_1 + 0.375\, \omega_2^2 a_2^3 \beta_8 + 0.25\, \omega_1^2 a_1^2 a_2 \beta_6 [1 + 0.5 \cos 2\lambda] + 0.375 [\omega_1\omega_2 a_1 a_2^2 \beta_7 + \omega_1^3 a_2^3 \beta_5/\omega_2] \cos\lambda \quad (15)$$

$$\dot{\delta}_2 = \{-0.125 [\omega_1^2 a_1^3 a_2 \beta_6 + \omega_2^2 a_1 a_2^3 a_7] \sin 2\lambda - 0.325 [\omega_1^3 a_1^4 \beta_5/\omega_2 + \omega_2^3 a_2^4 \alpha_8/\omega_1] \sin\lambda - 0.125\, \omega_1\omega_2 a_1^2 a_2^2 [\alpha_6 + \beta_7] \sin\lambda\}/(a_1 a_2) \quad (16)$$

where $\lambda = \varepsilon\sigma t - \delta_2$, $\dot{\lambda} = \varepsilon\sigma - \dot{\delta}_2$.

Steady-state amplitudes a_1 and a_2 and phase lag δ_2 can be obtained by applying the conditions that $\dot{a}_1 = \dot{a}_2 = \dot{\delta}_2 = 0$ in Eqs. (14), (15) and (16). Stability of the steady-state solution must be examined by considering the small perturbations at the solution point.

Examining Eq. (16), it is found that the possible solution sets of steady-state motion depend on two parameters β_5 and α_8 as shown in **Table 1**. For example, if both β_5 and α_8 are non-zero, both a_1 and a_2 must be non-zero in order that $\dot{\delta}_2 = 0$. This means that the single mode solutions ($a_1 = 0$, $a_2 > 0$) and ($a_1 > 0$, $a_2 = 0$) do not exist : all the solutions are the coexisting two modes in galloping ($a_1 > 0$, $a_2 > 0$), i. e. multi-mode galloping. On the other hand, if only α_8 is zero then the solution ($a_1 = 0$, $a_2 > 0$) exists, while if only β_5 is zero, the solution ($a_1 > 0$, $a_2 = 0$) will exist.

As seen here, the steady-state vibration mode in galloping is principally determined by the values of the parameters β_5 and α_8. These parameters are functions of mode shapes, wind velocity, cross-section and aerodynamic force coefficient (γ_1, γ_2, U, D and A_3, respectively) as defined in Eqs. (7·j) and (7·p). These parameters are zero when one mode shape is symmetric and the other mode shape is asymmetric. This property regarding the mode shape always observed in symmetric structures. On the other hand, these parameters are not zero, if the structure has unsymmetrically distributed mass or if the wind velocity and angle of attack are non-uniform along the structure axis or if the cross-section non-uniformly changes along the structure axis.

Then two types of bridge tower are employed as the case study. Firstly, the galloping behaviour of Higashi-Kobe bridge tower is studied. Note that this tower has symmetrically distributed mass. Next, this bridge tower is modified by adding a small mass at one leg of the tower to make the structure unsymmetric, i. e. β_5 and α_8 are not zero. Galloping behaviour of this modified tower is also investigated to study the multi-mode galloping. The modified tower can be considered as the model of tower with one climbing crane on its leg during construction.

4. GALLOPING BEHAVIOUR OF HIGASHI-KOBE BRIDGE TOWER

The three dimensional 1 : 100 scaled model of the Higashi-Kobe cable-stayed bridge tower with rectangular cross-section is employed as the case study. Modal selection in galloping of this bridge tower model exposed to smooth wind flowing along the bridge axis is analytically investigated.

Note that the model properties and modal properties are shown in **Fig. 1**. The generalized masses of both the first and the second modes are taken as unity. Since the exact wind force coefficients of this tower is not measured and the cross-section of tower's leg is similar to 2 : 3 rectangular cross-section, then the quasi-steady wind force of 2 : 3 rectangular cross-section obtained by Novak and Tanaka[8] is used.

Using its first two in-plane mode shapes, the following approximations hold :

$$\alpha_3=\alpha_6=\alpha_8=\beta_2=\beta_4=\beta_5=\beta_7=0 \quad (17)$$

With use of Eq. (17), Eqs. (14), (15) and (16) are reduced to :

$$\dot{a}_1=0.5\,a_1\alpha_1+0.375\,\omega_1^2a_1^3\alpha_5+0.25\,\omega_2^2a_1a_2^2\alpha_7[1+0.5\cos 2\lambda] \quad (18)$$

$$\dot{a}_2=0.5\,a_2\beta_1+0.375\,\omega_2^2a_2^3\beta_8+0.25\,\omega_1^2a_1^2a_2\beta_6[1+0.5\cos 2\lambda] \quad (19)$$

$$\dot{\delta}_2=-0.125[\omega_1^2a_1^2\beta_6+\omega_2^2a_2^2\alpha_7]\sin 2\lambda \quad (20)$$

In order that $\dot{\delta}_2=0$ in Eq. (20), the bracket term or the sinusoidal term must be zero. Since β_6 and α_7 always have the same sign (Eqs. (7·l) and (7·m)), the bracket term can not be zero. Then $\sin 2\lambda$ must be zero : $2\lambda=0$ or π and $\cos 2\lambda=1$ or -1, respectively, Solving Eqs. (18) and (19) with this condition, one obtains the following steady-state solutions.

set 1 : $a_1=0,\quad a_2=0,\quad \lambda=$arbitrary (21)

set 2 : $a_1=\sqrt{-4\alpha_1/3\alpha_5}/\omega_1,\quad a_2=0,\quad \lambda=$arbitrary (22)

set 3 : $a_1=0,\quad a_2=\sqrt{-4\beta_1/3\beta_8}/\omega_2,\quad \lambda=$arbitrary (23)

set 4 : $a_1=\sqrt{4(\alpha_7\beta_1-\alpha_1\beta_8)/3(\alpha_5\beta_8-\alpha_7\beta_6)}/\omega_1$

$a_2=\sqrt{4(\alpha_1\beta_6-\alpha_5\beta_1)/3(\alpha_5\beta_8-\alpha_7\beta_6)}/\omega_2,\quad \lambda=0$ (24)

set 5 : $a_1=\sqrt{4(\alpha_7\beta_1-3\alpha_1\beta_8)/(9\alpha_5\beta_8-\alpha_7\beta_6)}/\omega_1$

$a_2=\sqrt{4(\alpha_1\beta_6-3\alpha_5\beta_1)/(9\alpha_5\beta_8-\alpha_7\beta_6)}/\omega_2,\quad \lambda=\pi/2$ (25)

Stability of solution sets 1 to 5 is examined at various wind velocities. It was found that solution sets 1, 2 and 3 are stable at certain wind velocities while solution sets 4 and 5 are always unstable. Results of only the stable solutions for two representative values of λ, namely $\lambda=0$ and $\lambda=\pi/2$, are shown in **Fig. 4**, where U_{cr_1} and U_{cr_2} are the onset wind velocity for galloping of the first and the second modes $\left(U_{cr_i}=\xi_i\omega_iD/\left(n_iA_1\int\gamma_i^2dx\right)\right)$, respectively. The overlap area in **Fig. 4** (a) indicates that either the solution set 2 or 3 is stable. This area is the largest when λ is zero and it decreases as increase of λ. It vanishes when λ is equal to $\pi/2$.

The solid line in **Fig. 4** indicates the stable solutions for the specific bridge tower model shown in **Fig. 1**. Note that the computed onset wind velocity of the first mode is less than that of the second mode because $\xi_1\omega_1/\int\gamma_1^2dx$ is greater than $\xi_2\omega_2/\int\gamma_2^2dx$. It was indeed observed in the wind tunnel experiment that U_{cr_1} is greater than U_{cr_2}, i. e. $U_{cr_1}=2.5$ m/s and $U_{cr_2}=2.2$ m/s.

At the wind velocity less than the modal onset wind velocities, U_{cr_1} and U_{cr_2}, e. g. at point 1 in **Figs. 4** (a) and 4 (b), both modes are stable at zero amplitudes, i. e. no galloping. At point 2 with $U_{cr_2}<U<U_{cr_1}$, only the second mode is stable in galloping. At point 3 ($U>U_{cr_2}$, U_{cr_1}), the existence of the first mode or of the second mode in galloping is determined by the initial conditions.

Fig. 5 shows how the initial amplitudes, a_1 and a_2 and the initial phase lag λ affect the modal selection. If only the first mode excitation is given to the tower (indicated by point A) the response will reach stable

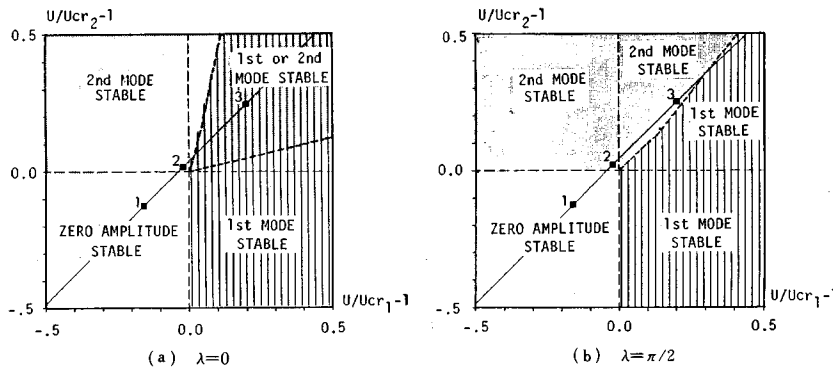

Fig. 4 Stability map of the tower with two representative values of phase lag, λ.

finite amplitude of a_1 with zero amplitude of a_2. Similarly, finite amplitude of a_2 with zero amplitude of a_1 is the stable galloping mode if only second mode excitation is given (point B). If both first and second mode excitations are simultaneously given to the tower, the stable galloping mode depends upon the initial amplitudes (a_1 and a_2) and the initial phase lag (λ). For example, if the tower starts to oscillate from point C in **Fig. 5**, the first mode's response dies out while the second mode's amplitude grows to steady-state, and *vice versa* for the case of point D. It is interesting to note that when initial phase lag given to the tower is nearly $\pi/2$ (point E), the first mode's amplitude will increase until it reaches saddle point, F then it decays to zero amplitude, while the second mode monotonically grows to the steady-state at point G ($a_1=0$, $a_2>0$).

It should be noted that the state space shows only the processes of the response to the steady-state. It does not give any information on the build-up time for the response to reach steady-state[9].

The observations in wind tunnel experiment using the 3-dimensional model of the Higashi-Kobe bridge tower can be interpreted by the analytical results as further presented below.

When the wind velocity was 2.3 m/s, galloping of the second mode appeared and the first mode galloping was not observed. This corresponds to point 2 in **Figs. 4(a)** and **4(b)**.

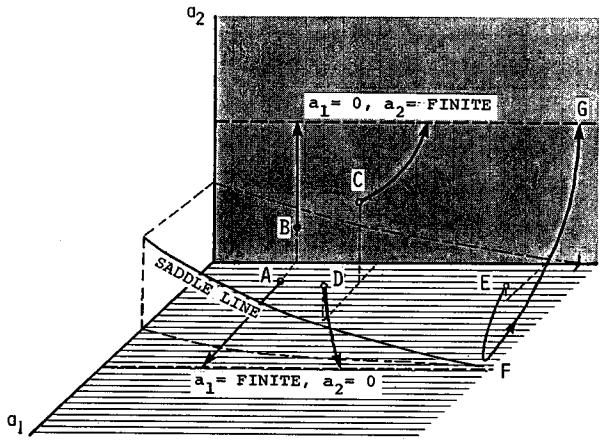

Fig. 5 State space of the tower at $U>U_{cr_1}$, U_{cr_2} (point 3 in Fig. 4).

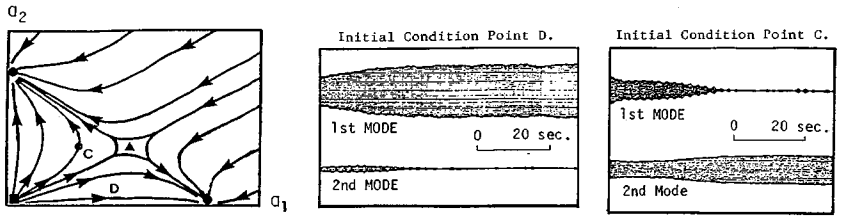

(a) Path of modal transient amplitudes and time history responses at initial phase lag $\lambda \neq \pi/2$

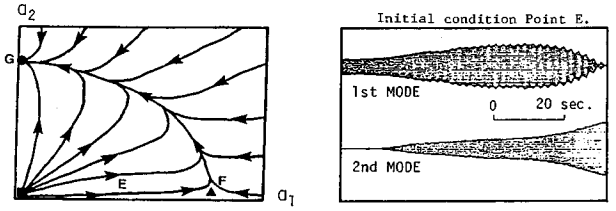

(b) Path of modal transient amplitudes and time history responses at initial phase lag $\lambda=\pi/2$

Fig. 6 Galloping responses of the tower's model observed in wind tunnel experiments (■ : unstable point, ▲ : saddle point and ● : stable node).

At higher wind velocity ($U>2.5$ m/s), galloping of first mode was also observed. Selection of the first mode or of the second mode in galloping depended upon the initial disturbances given to the tower as shown in Fig. 6(a). The left hand side figure presents the path of modal transient amplitudes which is similar to the phase plane, but phase lag λ is not constant in this figure, it changes along the path.

For the wind velocity greater than 2.9 m/s, the first mode initially appeared in galloping, but after sometime its amplitude decayed while the second mode increased and reached the steady-state motion as shown in Fig. 6(b). This phenomenon corresponds to point 3 in Fig. 4(b).

The observations in the wind tunnel experiment can be well explained by the present nonlinear analysis.

5. GALLOPING BEHAVIOUR OF MODIFIED HIGASHI-KOBE BRIDGE TOWER

The Higashi-Kobe cable-stayed bridge tower model in Fig. 1 was modified by adding a small concentrated mass at one leg of the tower. By adding this small mass, mode shapes are changed so that β_5 and α_8 are not zero. Mode shapes as well as structural properties of the modified tower are shown in Fig. 7. Cross-section of this modified tower, unlike the tower shown in Fig. 1 which is tapered cross-section, is uniform 2 : 3 rectangular cross-section.

Note that the generalized masses of both the first and the second mode equal to unit and that the values of all the parameters in Eq. (17) including β_5 and α_8 are non-zero.

Steady-state amplitude of the modified tower can be obtained by equating $\dot{a}_1$, $\dot{a}_2$ and $\dot{\delta}_2$ in Eqs. (14) to (16) to zero and solving these equations simultaneously.

Steady-state solutions and their stability are examined at various wind velocities. It was found that the solution of $a_1=0$ and $a_2=0$ is stable, i. e. no galloping, when the wind velocity is less than the onset wind velocities ($U<U_{cr_1}$, U_{cr_2}).

At higher wind velocities ($U>U_{cr_2}$), only multi-mode galloping is stable as shown in Fig. 8(a) ($U_{cr_2}<U<U_{cr_1}$) and Fig. 8(b) ($U>U_{cr_1}$, U_{cr_2}). It should be noted that in this tower U_{cr_2} is less than U_{cr_1} because $\xi_2\omega_2/\int\gamma_2^2dx$ is smaller than $\xi_1\omega_1/\int\gamma_1^2dx$. This was also confirmed in the wind tunnel experiment. Fig. 8 (a) is particularly interesting since galloping of the first mode is observed even the wind velocity is less than the first mode onset wind velocity, U_{cr_1}.

Fig. 8 also indicates that in the multi-mode galloping, the stable steady-state amplitude of the first mode is less than that of the second mode because the structural damping of the first mode is larger than that of the second mode. It is also found that each modal amplitude slightly changes according to the value of phase lag, λ, i. e. the stable solution depends on λ. The ratio of a_1 to a_2, firstly, will increase with the increase

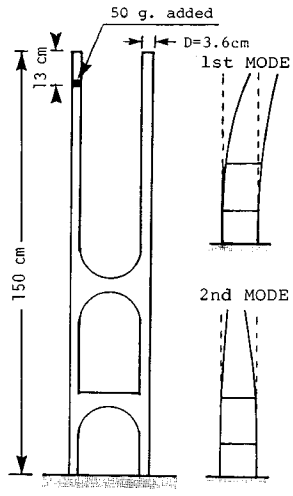

Modal circular natural frequencies
$\omega_1=40.7$ rad/s, $\omega_2=46.1$ rad/s.
Modal critical damping ratios
$\xi_1=0.0013$, $\xi_2=0.0012$.
Modal mass ratios
$n_1=n_2=0.0004$.
Wind force coefficients of 2 : 3 rectangular cross-section
$A_1=6.6$, $A_2=0.0$, $A_3=-118.9$.
Modal Integrals (γ_i : i-th mode shape)

$\int\gamma_1^2dx=17.1$, $\int\gamma_2^2dx=19.1$,
$\int\gamma_1^3dx=-22.6$, $\int\gamma_2^3dx=-26.0$,
$\int\gamma_1^2\gamma_2dx=4.6$, $\int\gamma_1\gamma_2^2dx=-15.2$,
$\int\gamma_1^4dx=35.0$, $\int\gamma_2^4dx=52.8$,
$\int\gamma_1^3\gamma_2dx=-12.1$, $\int\gamma_1\gamma_2^3dx=17.0$,
$\int\gamma_1^2\gamma_2^2dx=14.9$.

Fig. 7 Model dimensions and properties of the modified Higashi-Kobe bridge tower.

of wind velocity and, finally, this ratio will reach an asymptote, i.e. unit in this tower.

Example of phase plane of this modified tower at $U > U_{cr_1}$, U_{cr_2} is also shown in Fig. 9. The steady-state solutions are points A, B, C and D. Note that in this figure, a_2 at point B is not zero but it is very small compared with a_1 and *vice versa* at point C. The wind velocity in this figure differs from that in Fig. 8 (b).

In this figure, point A ($a_1=0$, $a_2=0$), i.e. no galloping, is unstable while points B and C are saddle points. Only point D (a_1, $a_2>0$), i.e. multi-mode galloping, is stable. This means that wherever the modified tower starts to gallop, the tower's response goes to a steady-state motion at point D.

Galloping behaviour of the modified tower model was also experimentally studied in the wind tunnel. It was confirmed that only the multi-mode galloping was observed. Time history responses at $U_{cr_2} < U < U_{cr_1}$ and at $U > U_{cr_1}$, U_{cr_2} are presented respectively in Figs. 10 (a) and 10 (b) which correspond to Figs. 8 (a)

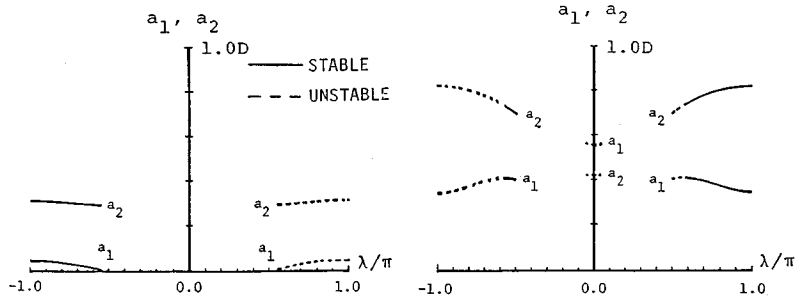

(a) $U_{cr_2} < U < U_{cr_1}$ (b) $U > U_{cr_1}$, U_{cr_2}

Fig. 8 Steady-state multi-mode solutions of the modified tower.

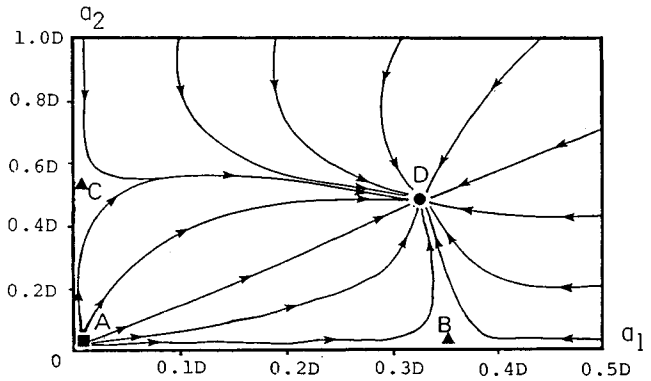

Fig. 9 Phase plane of the modified tower at $U > U_{cr_1}$, U_{cr_2} and phase lag $\lambda=0.7\,\pi$. (■ : unstable point, ▲ : saddle point and ● : stable node)

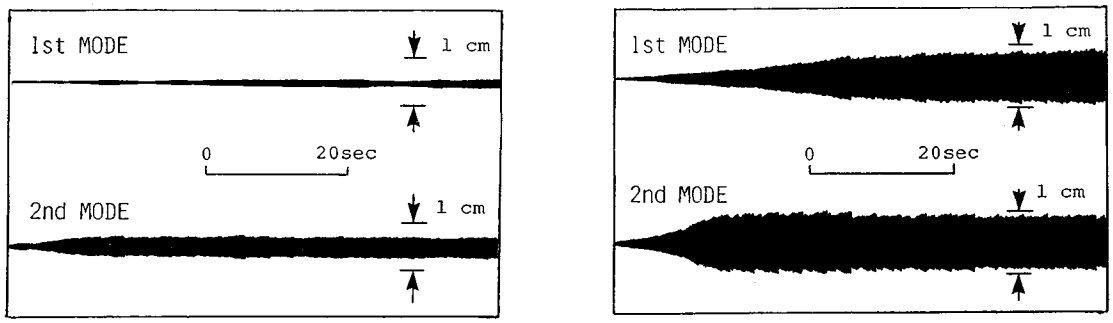

(a) $U=2.5$ m/s, $U_{cr_2} < U < U_{cr_1}$ (b) $U=2.9$ m/s, $U > U_{cr_1}$, U_{cr_2}

Fig. 10 Time history responses of the modified tower obtained from wind tunnel experiment (smooth wind flow).

and 8(b), respectively. In Fig. 10(b), galloping of the tower's model started from the rest position. Initially, the tower oscillated mainly in the second mode motion. As time passed the first mode motion gradually increased along with the second mode and finally it reached the multi-mode steady-state motions. The experimental results thus agree with the analytical results with respect to the coexistence of two modes in galloping.

Numerical integration also verifies the modal selection in galloping of the both types of bridge tower.

It should be noted that the computed galloping onset wind velocities very much differ from those observed in the experiments. For example, in the case of bridge tower's model shown in Fig. 1, the computed onset wind velodities are 0.071 m/s. and 0.068 m/s for that of the first mode and of the second mode, respectively, while the onset wind velocities observed in the wind tunnel test are 2.5 m/s and 2.2 m/s for that of the first mode and of the second mode, respectively. This means that the quasi-steady wind force is not applicable to this tower and that the unsteady wind force is suitable to employ. The quasi-steady assumption determines the wind force coefficients as the functions of angle of wind attack, i.e. implicit functions of structural velocity, while the unsteady wind force assumption determines the force coefficients as the functions of the reduced wind velocity and the structural amplitude, i.e. implicit functions of the structural velocity[10),11)]. The natural frequency of the second mode is close to that of the first mode, then the reduced wind velocity of the second mode is almost equal to that of the first mode. We are interested in the galloping behaviour of tower near the onset wind velocity. Therefore, in this narrow range of wind velocity, the unsteady wind force, which is also the function of reduced wind velodity, can be expressed approximately as the polynomial form of structural velocity, as shown in Eq. (3), but the force coefficients are, of course, different from those obtained from quasi-steady assumption. Then the results regarding modal selection in the galloping mode from this analysis are valid even when the unsteady wind force is assumed.

6. SUMMARY

Across-wind galloping of the proportionally-damped system having two closely-spaced natural frequencies was analytically and experimentally studied. The results from the nonlinear asymptotic analysis can be summarized as follows :

For structure having symmetric properties, galloping is the steady-state motion of a single mode, either in the first mode or in the second mode. Selection of the galloping mode depends upon the initial disturbances given to the structure.

For the structure having certain properties, such as unsymmetrically distributed mass or non-uniform cross-section, galloping is a motion in the two modes, i.e. multi-mode galloping. Modal steady-state amplitudes in multi-mode galloping slightly depends on the initial phase lag between the two modes.

ACKNOWLEDGMENTS

The authors would like to express their deepest thanks to Prof. Manabu ITO, Univ. of Tokyo for his valuable advice and encouragement throughout this study. Assistance provided by Mr. Izumi Shino, Univ. of Tokyo during the wind tunnel experiments is also fully acknowledged. The authors convey their thanks to Mr. Hiroshi Ishizaki, Hanshin Expressway Public Corporation for giving them opportunity for the wind tunnel testing of the Higashi-Kobe cable-stayed bridge tower. This study was partially supported by the Grant-in-Aids for Scientific Reserch, No. 61460156.

NOTATIONS

A_i : aeroelastic force coefficients
D : characteristic dimension of structure
$m(x)$: mass of structure per unit length
a_i : i-th modal steady-state amplitude
$F_Y(x, t)$: external wind force
n_i : i-th modal mass ratio

U : uniform wind velocity
$y_i(t)$: i-th modal response
β_i : parameters defined in Eqs. (7)
ξ_i : i-th modal critical damping ratio
σ : detuning parameter
ω_i : i-th modal circular natural frequency
U_{cri} : i-th modal onset wind velocity
$Y(x, t)$: response of structure
α_i : parameter defined in Eqs. (7)
$\gamma_i(x)$: i-th modal shape
ρ : air density
λ : phase lag

REFERENCES

1) Novak, M. : Aeroelastic Galloping of Prismatic Bodies, Journal of Engineering Mechanics Division, ASCE, EM1, pp. 115~142, Feb. 1969.
2) Blevins, R. D. and Iwan, W. D. : The Galloping Response of a Two-Degree-of-Freedom System, Journal of Applied Mechanics, Transaction of ASME, pp. 1113~1118, Dec. 1974.
3) Kasa, H. : Aeroelastic Behaviour of Cable-Stayed Bridge Tower, Graduation Thesis, University of Tokyo 1985 (in Japanese).
4) Phoonsak, P., Fujino, Y., Ito, M. and Shino, I. : Galloping in Two-Degree-of-Freedom System with Coalesced Natural Frequencies, Proc. of 9th National Symposium on Wind Engineering, Tokyo, Japan, pp. 187~192, Dec. 1986.
5) Phoonsak, P., Fujino, Y. and Ito, M. : Galloping of Tower-like Structure With Two Closely-spaced Natural Frequencies, Preprints of 7th International Conference on Wind Engineering, Aachen, West Germany, Vol. 5, pp. 29~38, Jul. 1987.
6) Phoonsak, P., Fujino, Y. and Ito, M. : Multi-mode Galloping of Bridge Tower With Two Closely-spaced Natural Frequencies, Proc. of 42nd Annual Conference of JSCE, pp. 680~681, Nov. 1987.
7) Shiraishi, N., Matsumoto, M., Shirato, H. and Ishizaki, H. : On Aerodynamic Stability Effects for Bluff Rectangular Cylinder by Their Corner-cut, Preprints of 7th International Conference on Wind Engineering, Aachen, West Germany, Vol. 2, pp. 263~272, Jul. 1987.
8) Novak, M. and Tanaka, H. : Effect of Turbulence on Galloping Instability, Journal of the Engineering Mechanics Division, ASCE, EM1, pp. 27~47, Feb. 1974.
9) Nayfeh, A. H. and Mook, D. T. : Nonlinear Oscillations, John-Wiley and Sons, New York, 1979.
10) Otsuki, Y., Washizu, K., Tomizawa, H. and Ohya, A. : A Note on The Aeroelastic Instability of A Prismatic Bar With Square Section, Journal of Sound and Vibration, Vol. 34, No. 2, pp. 233~248, 1974.
11) Washizu, K., Ohya. A., Otsuki, Y. and Fujii, K. : Aeroelastic Instability of Rectangular Cylinders In A Heaving Motion, Journal of Sound and Vibration, Vol. 59, No. 2, pp. 195~210, 1978.

(Received October 26 1987)